

Original Research Paper:

Biosynthesis Silver nanoparticles by using Supernatant *staphylococcus epidermidis* and antibacterial Activity of resistant pathogenic bacteria

Nisreen Wasmi Dawood¹

Maytham A. Al-Hamdani²

^{1,2}Department of Biology, College of Education for Pure Sciences, University of Basrah, Basrah, Iraq

Article history

Received: 15/05/20204

Revised: 26/06/2024

Accepted: 21/07/2024

*Corresponding Author: Nisreen Wasmi Dawood,

E-mail:

nissren.Wasmi.Daood@gmail.com

Abstract: Nanotechnology refers to the manipulation and fabrication of particles that are smaller than 100 nanometers in size in order to enhance the surface area. The area-to-volume ratio facilitates chemical interactions between individual atoms. The present work used a bacterial filtrate derived from *Staphylococcus epidermidis* bacterium and silver nitrate. The Gas chromatography–mass spectrometry analysis of the bacterial isolate extract identified many highly concentrated active chemicals, including methyl phenyl sulfoxide, 2, 3 Friedelin, and 1, 3, 5-triphenylcyclohexane. The UV-visible light spectrum of silver nanoparticles showed the highest absorbance peak at wavelength 416 nanometer, X-ray diffraction analysis showed four peaks at levels 111, 200, 220, and 311. The Fourier Transform Infrared Spectroscopy spectrum of the extracellular bacterial filtrate and the resulting silver particles showed several bands in the range 500-4000 cm⁻¹, which indicate O-H groups for alcoholic and phenolic compounds, N-H groups for amino acids, C=C for alkanes, and S= O belongs to sulfur compounds. Field-Emission Scanning Electron Microscope showed that silver nanoparticles are located within a nanoscale orbit. Their sizes reached 37.78-61.29 nanometers, with an average of 19.75 nanometers. Energy-dispersive X-ray spectroscopy, which accompanies the scanning electron microscope examination, recorded the weight percentage of silver as equal to 88%. Silver nanoparticles manufactured from the extract of *Staphylococcus epidermidis* bacteria were effective against multi-antibiotic-resistant pathogenic isolates. *Staphylococcus aureus* bacteria were more resistant, with an average diameter of inhibition of 11.11 mm. While *Pseudomonas aeruginosa* bacteria were more sensitive, with an average diameter of inhibition of 14.57 mm, the concentration of 200 µg/ml was the most effective.

Keywords: Supernatant bacterial, *Staphylococcus epidermidis*, Silver nanoparticles, GC-Ms, absorbance

1. Introduction

Supernatant bacterial, *Staphylococcus epidermidis*, Silver nanoparticles, GC-Ms, absorbance. There is

widespread concern about the health threat from air pollution and airborne antibiotic resistance genes (ARGs) [3]. [4] showed that bacterial aerosols are an important means of transmitting airborne pathogens to

the human host, which causes respiratory infections and allergic responses. Bacterial species have developed many mechanisms to survive stress Antibiotics [5]. The functional groups of modified antibiotics may have a common substrate, for example, ATP, transferable by covalent modification of the antibiotic by acetylation, phosphorylation, adenylation, nucleotidylation, ribosylation, or glycosylation. Moreover, changes in cell surface receptors, redox systems, and hydrolysis lead to multidrug resistance [6].

Nanoparticles are small particles that behave like a single unit based on their properties and methods of transport, They are classified according to their diameter into fine nanoparticles with a diameter ranging between (1000-2500) nanometers and super nanoparticles with a diameter of (1-100) nanometers[7].

2. Methodology

Preparation of Supernatant

Staphylococcus epidermidis bacteria were isolated from the air of Basrah Governorate, Iraq. It was diagnosed molecularly based on the 16sRNA gene. Then, using it in the manufacture of silver nanoparticles according to [8].

Gas mass chromatography-mass spectrometry (GC-Ms):

GC-Ms technology was used to detect compounds contained in the bacterial filtrate. After obtaining the spectrum for each compound, the results were processed with the Solution MS - GC program. In addition, identifying pikas according to what is stated in the library database [9].

Silver nanoparticles

Add 1 ml of silver nitrate to 10 ml of the bacterial filtrate. A concentration of 1 molar was obtained by mixing the two solutions using a magnetic stirrer at a temperature of 80 °C. So, after 20 minutes, the pale yellow color began to change to a reddish

brown color, which stabilized after 60 minutes. The solution was then centrifuged to separate impurities (8000 rpm) for 20 minutes. The precipitate was taken, washed with distilled water three times, and dried in an oven at 50°C to obtain a powder

of silver nanoparticles, Figure (1)



B- Extract after adding silver nitrate A-Extract before adding silver nitrate Figure1. Synthesis of silver nanoparticles by bacterial aqueous extract.

Silver of Characterization Nanoparticles by Biosynthesis

The properties of AgNPs nanoparticles formed from the reduction of silver ions by Staphylococcus epidermidis bacterial extract were studied through the following tests.

UV-Vs Spectral Analysis

The absorbance of the resulting solutions confirms the presence of nanoparticles. Therefore, 3 ml of nanosilver solution was taken after dilution with deionized water. It was placed in the quartz cell of the spectrometer in the range of 200-800 nanometers. Filtering is done with distilled water. This analysis was conducted at the Al-Amin Center for Research and Life Technologies at the Holy Shrine of the Holy Shrine, Najaf Al-Ashraf - Iraq.

X-ray Diffraction (XRD) Analysis

This analysis provides the long-range order, i.e., structure, for crystalline materials and the short-range order for non-crystalline materials. From this information, we deduce the network constants and

phases, the average grain size, and the degree of crystallinity. The average crystalline or grain size was calculated using the Scherer equation: $D = (K\lambda/\beta 1/2 \cos \theta)$

Field emission scanning electron microscopy (FESEM)

To examine the surface morphology of silver nanoparticles, it was ground to prepare for examination with a scanning electron microscope after turning it into a colloidal suspension. Then a drop of it is added to the carbon holder to be inserted into the device at a distance of 10.2 mm and a voltage of (12.5-15) KV. The nanoparticle size was determined using ImageJ software [10]. The analysis was conducted at the Ministry of Science and Environment - Baghdad, Iraq.

Energy -Dispersive X-ray Spectroscopy (EDX)

This analysis is important for detecting nanoelements in the study sample [11]

Fourier transform infrared spectroscopy (FTIR).

Infrared spectroscopy analysis is an effective tool used to determine the functional groups present in the bacterial extract and silver nanoparticles. The vibration modes of the chemical bonds present in the bacterial filtrate solution and the nanosilver solution were analyzed. The functional groups have been registered in a scope. (cm - 1500 - 4000) This analysis was conducted at the Research Center - University of Tehran - Iran.
Antimicrobial Activity of AgNPs:

In order to detect the effect of silver nanoparticles on resistant bacterial isolates, we followed the agar well diffusion methods and agar well diffusion methods according to [12].

Statistical analysis

Quantitative data were represented by arithmetic mean \pm standard deviation (SD) and compared with one-way ANOVA. Then, a multivariate analysis of variance test (MANOVA) according to the least significant difference (LSD) test. The results were compared with a probability level of less than 0.05 [13].

3. Results & Discussion

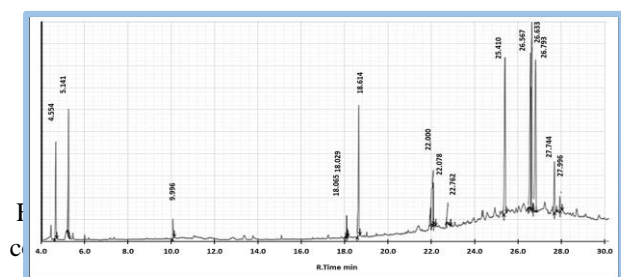
The active compounds of the bacterial extract of *Staphylococcus epidermidis* isolate were determined by GC-MS technology.

The results of gas-contact mass spectrometry analysis revealed that the bacterial extract of the *Staphylococcus epidermidis* isolate contained the presence of compounds at different concentrations. The number reached nine vehicles. The highest concentration was 15.35%, represented by the compound 2,3- Diphenylcyclopropyl methyl phenyl sulfoxide. It is followed by the compound Friedelin, with a concentration of 14.59%. Then, the compound 1,3,5-triphenylcyclohexane, with a concentration of 10.45%, as in Figure 2 and Table 1.

Many previous studies have shown a wide number of compounds available in bacterial extracts that may contribute to the reduction of silver ions and the encapsulation of nanoparticles. [14] revealed a group of effective compounds as well as their role as antioxidants and anti-inflammatory agents. In addition to its role in biotechnology, such as agriculture, medicine, and many others, as revealed by [15] identified nine active compounds using GC-MS technology. [16] indicated the presence of 231 secondary metabolites belonging to 26 bacterial strains of the genus *Bacillus subtilis*.

The compound Diphenylcyclopropyl methyl phenyl sulfoxide (is known to be an antioxidant carboxylic acid. It is considered a treatment for skin rashes and bruises. [17]. This compound constituted the largest percentage, which may be due to its vital activity in encapsulating silver ions.

The Friedelin compound has important pharmacological effects. It is antimicrobial, antioxidant, anti-cancer, and liver-protective. In addition to its role as an anti-diabetic agent, it is also considered an insect repellent and a good herbicide. It prevents the metabolism process, and thus, fertilin provides potential materials for the manufacture of medicines [18]. The third compound is 1, 3, 5-triphenylcyclohexane, which [19] referred to as antimicrobial.



peak	R-time	Chemical Name	Aeara%	Molecular Formula	Molecular Weight
1	4.554	Pentanone, 4-hydroxy-4--2 me	6.00	C6H12O2	116
2	5.141	Styrene	6.33	C8H8	104
3	9.996	Triethyl phosphate	1.08	C6H15O4	182
4	18.029	Cyclobutane, 1,3-diphenyl-, tr	2.79	C16H16	208
5	18.065	Cyclopropylphenylmethane	1.36	C10H12	132
6	18.614	Benzene, 1,1'-(1,2-cyclobutan	9.54	C16H16	208
7	22.000	Cholestane	5.53	C27H48	372
8	22.078	(2,3-Diphenylcyclopropyl)me	4.68	C22H20OS	332
9	22.762	(2,3-Diphenylcyclopropyl)me	3.00		
10	25.410	Cyclohexane, 1,3,5-triphenyl:	10.45	C24H24:	312
11	26.567	Friedelan-3-one	14.59	C30H50O:	426:
12	26.633	(2,3-Diphenylcyclopropyl)me	15.35		332
13	26.793	(2,3-Diphenylcyclopropyl)me	14.14	C22H20OS	332
14	27.744	(2,3-Diphenylcyclopropyl)me	3.76		332
15	27.996	(2,3-Diphenylcyclopropyl)me	1.39		116

Table 1. Active compound in the bacterial extract of the isolate *Staphylococcus epidermidis*

UV-visible analysis spectrometry

Ultraviolet spectroscopy analysis proves that nanoparticles have exceptional optics that are linked to their shape and size, making them interact with specific wave frequencies of light [20]. The silver nitrate reductase enzyme in the bacterial cell wall has an important role in reducing Ag⁺ to Ag⁰, in addition to its role as a stabilizing and covering agent [21], which in turn leads to the formation of the phenomenon of surface plasmon resonance (SPR), or what is called Mie resonance, which leads to color change [22]. The highest wavelength appeared at 416 nm, Figure (3). Many studies revealed the highest absorption peak, as [23] indicated the highest absorption peak at 415 nm.

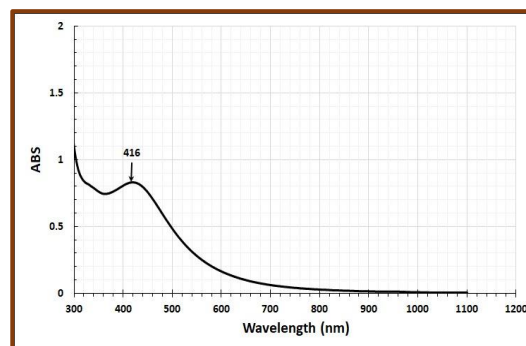


Figure 3. UV-Vis spectroscopy analysis of a solution of silver nanoparticles synthesized from the bacterial extract *Staphylococcus epidermidis*

X-ray diffraction:

The results of X-ray diffraction analysis of nanoparticles synthesized from the bacterial extract *Staphylococcus epidermidis* showed the appearance of four peaks in Figure (4) at the angle 2θ, represented by (38.093, 44.894, 64.593, 77.704), which correspond to the values (311, 220, 200, 111), respectively. Joint committee powder diffraction standards JCPDS 04–0783. A number of peaks preceding the 20° angle were observed, believed to be the result of crystallized bioorganic phases on the surface of AgNPs [24]. By applying Scherer's Formula, the crystallite size was found to be equal to 19.57 nanometers.

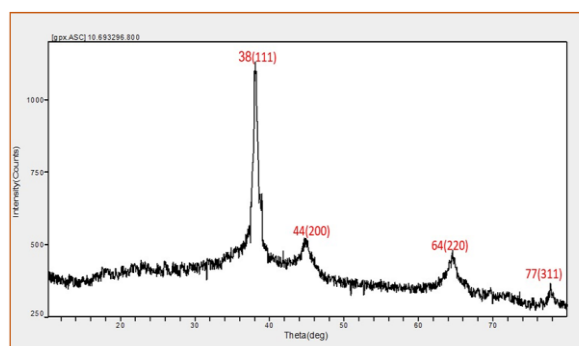


Figure 4. X-ray diffraction spectrum of silver nanoparticles synthesized by *Staphylococcus epidermidis*

Field emission scanning electron microscopy (FESEM)

The results of the scanning electron microscope analysis

of silver nanoparticles synthesized from the aqueous bacterial extract of *Staphylococcus epidermidis* revealed spherical shapes with a size ranging between (37.78 - 61.29) nanometers, falling within the nanoscale range, as shown in Figure (5).

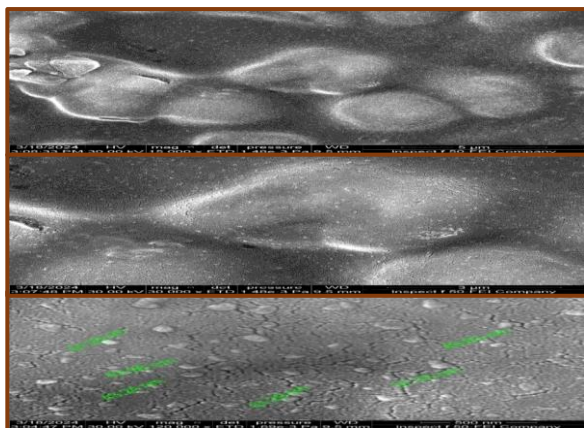


Figure 5. Silver nanoparticles synthesized from aqueous bacterial extract of *Staphylococcus epidermidis*, measuring 500, 3, and 5 nm, respectively.

Energy -Dispersive X-ray Spectroscopy (EDX)

Energy dispersive X-ray spectroscopy confirmed the presence of silver, as its weight percentage was Wt. %, 88%. The high-intensity absorption peak was at 3 keV, which is the standard location for the appearance of the silver element (Figure 6) due to surface plasmon resonance (SPR). Which confirms the presence of nanocrystalline silver [25].

The presence of other elements, such as Al and Au, observed in the EDX spectrum may be due to the carbon grid that was used during sample preparation [26].

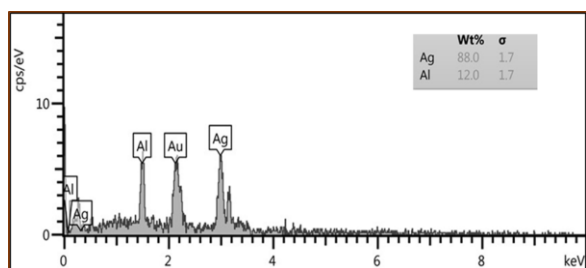


Figure 6. X-ray energy scattering diagram of silver

nanoparticles synthesized from *Staphylococcus epidermidis* extract

Fourier transform infrared spectroscopy (FTIR)

Infrared spectroscopy analysis of *Staphylococcus epidermidis* bacterial aqueous extract and silver nanoparticles was conducted. Many absorption peaks appeared within a spectral range ranging from (500-3854) cm^{-1} . If it is proven that it is due to the effective totals of those compounds resulting from the extract after they were compared to the standard packages [27].

These biomolecules from the bacterial extract may have a role in reducing silver nitrate to nanosilver and coating it [28]; [29]. Figure (7) shows the appearance of absorption bands between (581-777) cm^{-1} , where A indicates the C-H chain, which means the aliphatic alkane group and the 920 cm^{-1} band indicates the group of alkanes with the C=C chain.

Absorption bands between (1023-1082) cm^{-1} indicate groups of phenols with a C-O bond. Bands 1148 cm^{-1} indicate organic sulfur groups with an S=O bond. The band 1396 cm^{-1} indicates groups of alcohols and carboxylic acids with an O-H bond. The 1516 cm^{-1} band is represented by nitro groups that have the N-O bond.

The band 1570 cm^{-1} indicates groups of alkenes with the C=C chain, the band 2313 cm^{-1} represents the organic sulfur groups with the S-H chain. The band 2945 cm^{-1} represents the groups of aliphatic alkanes with the C-H chain. Figure (8): Absorption peaks appeared represented by aliphatic alkanes ranging from (555-748) cm^{-1} with the C-H bond. The band 1020 cm^{-1} represents the amine group with the C-N bond.

Band 1123 cm^{-1} with the S=O chain represents the organic sulfur group (sulfone), absorption band 1263 cm^{-1} indicates the phenol group with the C-O chain, band 1398 cm^{-1} represents the fluorine group with the C-F chain, band 1524 with the N-O chain indicates the absorption group. Nitro, band 1645 cm^{-1} represents groups of alkenes with a C=C bond.

The band 1645 cm^{-1} represents the groups of alkenes

with the C=C bond. The band 3429 cm⁻¹ represents the amine group with the N-H link. The spectral range is between (3738-3854) cm⁻¹, represented by the O-H bond, indicating groups of alcohols and carboxylic acids. The proteins of the bacterial extract can bind to the free amino group or cysteine residue. Therefore, the stabilization of AgNPs by proteins has become a clear result [30].

Proteins have a high ability to bind nanoparticles through electrostatic forces of attraction with the negatively charged carboxyl groups present in the enzyme [31].

The functional groups, represented by C-O, C-C, and C=C, derived from the proteins present in the biomolecules of the extract, bind to the surface of the nanoparticles to protect them from aggregation or agglomeration[32].

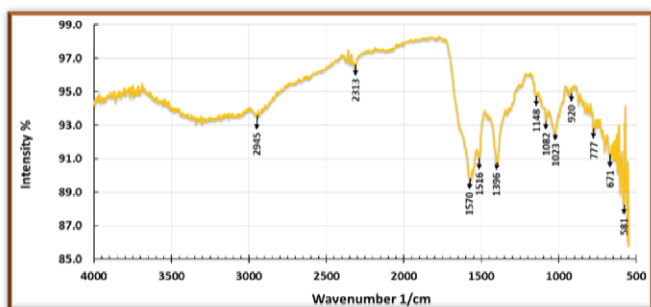


Figure 7. Infrared spectrum of bacterial extract *Staphylococcus epidermidis*

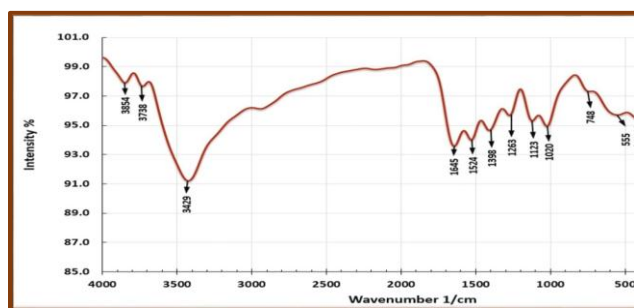


Figure 8. Infrared spectrum of silver nanoparticles synthesized from *Staphylococcus epidermidis* extract

Study of the antibacterial effectiveness of silver nanoparticles synthesized from the bacterial extract Staphylococcus epidermidis

The results of testing the biological effectiveness of biosynthetic particles from the bacterial extract *Staphylococcus epidermidis* by well diffusion method on Mueller-Hinton medium against the six isolates with multiple antibiotic resistance, *P. aeruginosa*, showed. *E. coli*, *S. typhi*, *S. aureus*, *S. pneumonia*, and *E. faecalis*, where there were significant differences in the rate of inhibition of the diameters of the pathogenic isolates when treated with the concentrations used of 50, 100, and 200 micrograms/ml.

The concentration of 200 µg/ml had a clear effect on all six pathogenic isolates at a rate of 20.33 mm. At the concentration of 50 µg/ml, the lowest rate of inhibition appeared, amounting to 6.83 mm. It was clear from the results of the statistical analysis that the bacterial isolate *S. aureus* recorded the lowest rate of inhibition diameter, which reached 11.11 mm, while the bacterial isolate *p. aeruginosa*. The highest rate of inhibition diameter is 14.57 mm Table (2).

Table 2. Antibacterial effectiveness of silver nanoparticles synthesized from *Staphylococcus epidermidis* bacterial extract

concentrations isolates	50 µg/mL	100 µg/mL	200 µg/mL	Mean /ml	Multivariate
<i>Streptococcus pneumoniae</i>	8.33±1.15	10.00±2.00	16.00±2.00	11.44	LSD= 3.048 p= 0.001*
<i>Staphylococcus aureus</i>	5.67±1.53	9.00±2.00	18.67±1.53	11.11	
<i>Enterococcus faecalis</i>	6.00±2.00	9.67±0.58	20.67±2.08	12.11	
<i>Escherichia coli</i>	7.00±2.00	10.33±1.53	21.33±3.51	12.89	
<i>Salmonella typhi</i>	4.67±1.53	13.0±1.73	20.67±1.53	12.78	
<i>Pseudomonas aeruginosa</i>	9.33±1.15	9.67±1.53	24.67±2.08	14.57	
mean	6.83	10.28	20.33		
Effect of isolates	LSD= 1.76 p=0.005*				
Effect of concentrations	LSD= 1.245 p=0.0001**				

[33] indicated that the effect of biosynthetic silver nanoparticles on Gram-negative bacterial isolates was higher compared to Gram-positive bacterial isolates. The reason may be due to the difference in the structure and molecular components of the peripheral cell wall between Gram-positive and Gram-negative bacteria, especially with regard to the membrane and cell wall structure (Figure 9), (10).



Figure 9. bioactivity of silver nanoparticles synthesized from *Staphylococcus epidermidis* bacterial extract against pathogenic Gram- positive bacterial species

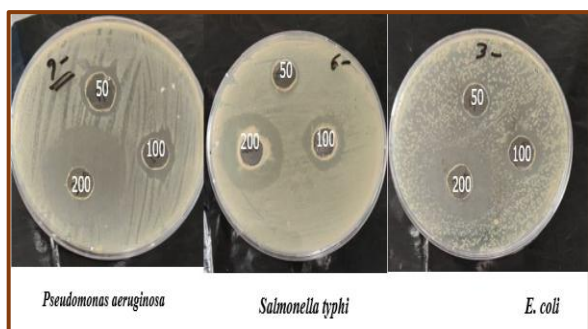


figure 10. bioactivity of silver nanoparticles synthesized from *Staphylococcus epidermidis* bacterial extract against pathogenic Gram-negative bacterial species

Conclusion

Antibiotic resistant bacteria have been continuously increasing over the past decade; hence, there is a need to detect another method to overcome this problem. In the present scenario, AgNPs have appeared as a promising antibacterial candidate in the medical field. Hence it could be potentially applied in the fabrication of silver impregnated antimicrobial materials for biomedical applications. We have demonstrated green process for the synthesis of silver nanoparticles from *Staphylococcus epidermidis* Within 60 minutes of time, spherical shaped nanoparticles from (37.78 - 61.29) nm size were formed.

The method described is highly efficient and cost effective to produce silver nanoparticle. Based on the results from this study, we can deduce that biologically synthesized AgNPs may function by binding to Thiol (SH) groups of membrane proteins, enzymes, and phosphate groups of DNA, and can be efficiently used as antimicrobial agents.

References

1. Barhoum, A., García-Betancourt, M. L., Jeevanandam, J., Hussien, E. A., Mekkawy, S. A., Mostafa, M., ... & Bechelany, M. (2022). Review on natural, incidental, bioinspired, and engineered nanomaterials: history, definitions, classifications, synthesis, properties, market, toxicities, risks, and regulations. *Nanomaterials*, 12(2), 177. <https://doi.org/10.3390/nano12020177>.
2. Bahadar, H., Maqbool, F., Niaz, K., & Abdollahi, M. (2016). Toxicity of nanoparticles and an overview of current experimental models. *Iranian biomedical journal* 20(1),1. <https://doi:10.7508/ibj.2016.01.001>.
3. Li, N.; Chai, Y.; Ying, G.-G.; Jones, K. C., and Deng, W.-J. (2020). Airborne antibiotic resistance genes in Hon Kong kindergartens *Environmental Pollution* 260(5)114009. <https://doi.org/10.1016/j.envpol.2020.114009>.
4. Ribeiro, E.; Mira, A. R.; Ponte, T., and Oliveira, K. (2022). Airborne transmission of bacteria bioburden. In *Viruses, Bacteria and Fungi. in the Built Environment* (127-145): Elsevier. <https://doi.org/10.1016/B978-0-323-85206-7.00014-9>.

5. Windels, E. M.; Van den Bergh, B., and Michiels, J. (2020). Bacteria under antibiotic attack: Different strategies for evolutionary adaptation. *PLoS pathogens*, *16*(5), 1008431. <https://doi.org/10.1371/journal.ppat.1008431>
6. Rajivgandhi, G., Maruthupandy, M., Muneeswaran, T., Anand, M., & Manoharan, N. (2018). Antibiofilm activity of zinc oxide nanosheets (ZnO NSs) using *Nocardiosis* sp. GRG1 (KT235640) against MDR strains of gram negative *Proteus mirabilis* and *Escherichia coli*. *Process Biochemistry*, *67*(4), 8-18. <https://doi.org/10.1016/j.procbio.2018.01.015>.
7. Khan, S., and Hossain, M. K. (2022). Classification and properties of nanoparticles. In *Nanoparticle-based polymer composites* (15-54): Elsevier. <https://doi.org/10.1016/B978-0-12-824272-8.00009-9>.
8. Hassan, H. H. (2018). Biosynthesis and characterization of Ag Nanoparticles from *Klebsiella pneumoniae*. (PhD Thesis), University of Kufa, 158.
9. McNair, H. M., Miller, J. M., & Snow, N. H. (2019). Basic gas chromatography. *John Wiley & Sons*.
10. Dobson, E. T., Cimini, B., Klemm, A. H., Wählby, C., Carpenter, A. E., & Eliceiri, K. W. (2021). ImageJ and CellProfiler: Complements in Open- Source Bioimage Analysis. *Current protocols*, *1*(5), 89. <https://doi.org/10.1002/cpz1.89>
11. Ahamad, I., Aziz, N., Zaki, A., & Fatma, T. (2021). Synthesis and characterization of silver nanoparticles using *Anabaena variabilis* as a potential antimicrobial agent. *Journal of Applied Phycology*, *33*, 829-841.
12. Hetta, H. F.; Al-Kadmy, I. M.; Khazaal, S. S.; Abbas, S.; Suhail, A.; El-Mokhtar, M. A.; Ellah, N. H. A.; Ahmed, E. A.; Abd-Ellatief, R. B., and El-Masry, E. A. (2021). Antibiofilm and antivirulence potential of silver nanoparticles against multidrug-resistant *Acinetobacter baumannii*. *Scientific reports*, *11*(1), 10751. <https://doi.org/10.1038/s41598-021-90208-4>.
13. Ellersieck, M., and La Point, T. (2020). Statistical analysis. In *Fundamentals of Aquatic Toxicology* (307-343): CRC Press.
14. Mertler, C. A., Vannatta, R. A., & LaVenia, K. N. (2021). Advanced and multivariate statistical methods: *Practical application and interpretation*. *Routledge*. <https://doi.org/10.4324/9781003047223>.
15. Makuwa, S. C., & Serepa-Dlamini, M. H. (2021). The antibacterial activity of crude extracts of secondary metabolites from bacterial endophytes associated with *Dicoma anomala*. *International Journal of Microbiology*, *2021*(1), 12. <https://doi.org/10.1155/2021/8812043>
16. Anantha, P. S., Deventhiran, M., Saravanan, P., Anand, D., & Rajarajan, S. (2016). A comparative GC-MS analysis of bacterial secondary metabolites of *Pseudomonas* species. *The Pharma Innovation*, *5*(4), 84-89.
17. Kai, M. (2020). Diversity and distribution of volatile secondary metabolites

- throughout *Bacillus subtilis* isolates. *Frontiers in Microbiology*, 11, 478645. <https://doi.org/10.3389/fmicb.2020.00559>.
18. Gothai, S., Vijayarathna, S., Chen, Y., Kanwar, J. R., Wahab, H. A., & Sasidharan, S. (2018). In vitro-scientific evaluation on anti-*Candida albicans* activity, antioxidant properties, and phytochemical constituents with the identification of antifungal active fraction from traditional medicinal plant *Couroupita guianensis* Aubl. Flower. *Flower. J. Complement. Med. Res*, 8 (2) ,85-101.
 19. Singh, S. K., Shrivastava, S., Mishra, A. K., Kumar, D., Pandey, V. K., Srivastava, P., ... & Baek, K. H. (2023). Friedelin: Structure, Biosynthesis, Extraction, and Its Potential Health Impact. *Molecules*, 28(23), 7760. <https://doi.org/10.3390/molecules28237760>.
 20. Vanitha, V., Vijayakumar, S., Nilavukkarasi, M., Punitha, V. N., Vidhya, E., & Praseetha, P. K. (2020). Heneicosane—A novel microbicidal bioactive alkane identified from *Plumbago zeylanica* L. *Industrial Crops and Products*, 154, 112748. <https://doi.org/10.1016/j.indcrop.2020.112748>.
 21. Patil, R. B., & Chougale, A. D. (2021). Analytical methods for the identification and characterization of silver nanoparticles: A brief review. *Materials Today: Proceedings*, 47, 5520-5532. <https://doi.org/10.1016/j.matpr.2021.03.384>.
 22. Roy, A., Bulut, O., Some, S., Mandal, A. K., & Yilmaz, M. D. (2019). Green synthesis of silver nanoparticles: biomolecule-nanoparticle organizations targeting antimicrobial activity. *RSC advances*, 9(5), 2673-2702.
 23. Aswini, A., Jenifer, S., Ashina, J. N. B., Jeba Raj, Y., & Subashkumar, R. (2024). Fabrication of biogenic silver nanoparticles using *Bacillus vietnamensis* JA01: characterization and antibacterial activity. *Biomass Conversion and Biorefinery*, 1-8.
 24. Mondal, A. H., Yadav, D., Ali, A., Khan, N., Jin, J. O., & Haq, Q. M. R. (2020). Anti-bacterial and anti-candidal activity of silver nanoparticles biosynthesized using *Citrobacter* spp. MS5 culture supernatant. *Biomolecules*, 10(6), 944. <https://doi.org/10.3390/biom10060944>.
 25. Giri, A. K., Jena, B., Biswal, B., Pradhan, A. K., Arakha, M., Acharya, S., & Acharya, L. (2022). Green synthesis and characterization of silver nanoparticles using *Eugenia roxburghii* DC. extract and activity against biofilm-producing bacteria. *Scientific Reports*, 12(1), 8383. <https://doi.org/10.1038/s41598-022-12484-y>.
 26. John, M. S., Nagoth, J. A., Ramasamy, K. P., Mancini, A., Giuli, G., Natalello, A., ... & Pucciarelli, S. (2020). Synthesis of bioactive silver nanoparticles by a *Pseudomonas* strain associated with the antarctic psychrophilic protozoon *Euplotes focardii*. *Marine drugs*, 18(1), 38.
 27. Alsharif, S. M., Salem, S. S., Abdel-Rahman, M. A., Fouda, A., Eid, A. M., Hassan, S. E. D., ... & Mohamed, A. A.

- (2020). Multifunctional properties of spherical silver nanoparticles fabricated by different microbial taxa. *Heliyon*, 6(5), E03943.
<https://doi.org/10.1016/j.heliyon.2020.e03943>.
28. Al-Saadi, Abbas Khamas. (2021) Diagnosis and characterization of nanomaterials. 1st edition, Dar Al-Amir for Printing, Publishing and Distribution. Baghdad, Iraq.
29. Zhang, Z., Li, S., Gu, X., Li, J., & Lin, X. (2019). Biosynthesis, characterization and antibacterial activity of silver nanoparticles by the Arctic anti-oxidative bacterium *Paracoccus* sp. Arc7-R13. *Artificial cells, nanomedicine, and biotechnology*, 47(1), 1488-1495.
<https://doi.org/10.1080/21691401.2019.1601631>.
30. Mikhailova, E. O. (2020). Silver nanoparticles: Mechanism of action and probable bio-application. *Journal of functional biomaterials*, 11(4), 84-32.
<https://doi.org/10.3390/jfb11040084>.
31. Mohd Yusof, H., Abdul Rahman, N. A., Mohamad, R., & Zaidan, U. H. (2020). Microbial mediated synthesis of silver nanoparticles by *Lactobacillus Plantarum* TA4 and its antibacterial and antioxidant activity. *Applied sciences*, 10(19), 6973.
<https://doi.org/10.3390/app10196973>.
32. Sidhu, A. K.; Verma, N., and Kaushal, P. (2022). Role of biogenic capping agents in the synthesis of metallic nanoparticles and evaluation of their therapeutic potential. *Frontiers in Nanotechnology*, 3(1), 801620.
<https://doi.org/10.3389/fnano.2021.801620>.
33. Abarca-Cabrera, L.; Fraga-García, P., and Berensmeier, S. (2021). Bio-nano interactions: binding proteins, polysaccharides, lipids and nucleic acids onto magnetic nanoparticles. *Biomaterials research*, 25(12), 2-18.
<https://doi.org/10.1186/s40824-021-00212-y>.